European Journal of Medicinal Chemistry 44 (2009) 4758–4763

Contents lists available at ScienceDirect

European Journal of Medicinal Chemistry

journal homepage: http://www.elsevier.com/locate/ejmech

Short communication

Unusual cellular uptake of cytotoxic 4-hydroxymethyl-3-aminoacridine

Paul Peixoto [a], Walid Zeghida [b], Danièle Carrez [c], Ting-Di Wu [c], Nicole Wattez [a], Alain Croisy [c], Martine Demeunynck [b,*], Jean-Luc Guerquin-Kern [c], Amélie Lansiaux [a,**]

[a] Inserm U837, Centre Oscar Lambret, Université Lille Nord de France, Faculté de médecine de Lille, IRCL and IMPRT
[b] Département Chimie Moléculaire, UMR 5250, CNRS/Université Joseph Fourier, BP 53, 38041 Grenoble Cedex 9, France
[c] INSERM U759, Centre Universitaire; 91405 Orsay and Centre de Recherche de l'Institut Curie, Laboratoire Raymond Latarjet, Bat. 112, Centre Universitaire, 91405 Orsay cedex, France

ARTICLE INFO

Article history:
Received 29 December 2008
Received in revised form
3 June 2009
Accepted 29 June 2009
Available online 4 July 2009

Keywords:
Acridine
Antitumor agents
Cell distribution
Lysosomes
Real time fluorescence microscopy
Dynamic SIMS imaging

ABSTRACT

Aminoacridine derivatives display interesting chemical and biological properties in the field of antitumor agents. The synthesis of 4-hydroxymethyl-3-aminoacridine and its iodo labelled analogue allows the study of cell distribution using two innovative, complementary and powerful techniques, real time fluorescence microscopy and dynamic secondary ion mass spectrometry (SIMS). All the data point to lysosomal localization of the active molecule.

© 2009 Elsevier Masson SAS. All rights reserved.

1. Introduction

Acridine derivatives have a long story in the field of drug design and in particular as antitumor agents [1]. We have previously described a series of ortho-hydroxymethyl aminoacridines displaying interesting chemical and biological properties in the field of antitumor agents [2]. The most active compounds **1** and **2** (Fig. 1) are cytotoxic at nanomolar concentrations against various human cancer cell lines. These molecules interact with DNA by intercalation between base pairs and covalently bind to the macromolecule. Solvolytic studies pointed to the intermediate formation of highly electrophilic quinone-imine-methide species under general acid–base catalysis [3]. From these *in vitro* studies it was concluded that the molecules behave as typical DNA intercalating-alkylating agents. However, unlike most antitumor acridines that are topoisomerase inhibitors [4,5], compounds **1** and **2** do not interfere with topoisomerase activity (Fig. 1).

To assess the mode of action of compounds **1** and **2**, we took advantage of the intrinsic fluorescence of aminoacridine derivatives to visualize their cell distribution by confocal microscopy [2]. The results are interesting and different between compounds. The most potent molecule, compound **1**, did not distribute in the nucleus but was found as aggregates in the cytoplasm. However, compound **2**, which only differs by the presence of the carbamate group at the C-6 position of the acridine ring, showed a different behaviour, with a diffuse distribution in both the cytoplasm and the nucleus. Because these molecules have an *in vitro* mechanism of action different from the other acridine derivatives, and are fluorescent and cellularly active, it seemed important to understand these particularities notably by studying more finely their cellular localization. In the present article we report our cell distribution study of the most potent molecule **1**, using two innovative, complementary and powerful techniques, the secondary ion mass spectrometry (SIMS microprobe) and the real time fluorescence microscopy. The SIMS methodology requires the presence on the molecule of interest of an atom not found in living cells. In this purpose, we have prepared and studied the 6-iodo analogue of **1**.

2. Results and discussion

Aminoacridines display interesting chemical and biological properties in the field of antitumor agents, some of them are notably topoisomerase inhibitors [4,5]. On the other hand, the acridines that we synthesized (4-hydroxymethyl-3-aminoacridine derivatives),

* Corresponding author. Tel.: +33 476 514429; fax: +33 476 514946.
** Corresponding author. Tel.: +33 320 295953; fax: +33 320 169229.
E-mail addresses: martine.demeunynck@ujf-grenoble.fr (M.D. Demeunynck), a-lansiaux@o-lambret.fr (A. Lansiaux).

0223-5234/$ – see front matter © 2009 Elsevier Masson SAS. All rights reserved.
doi:10.1016/j.ejmech.2009.06.034

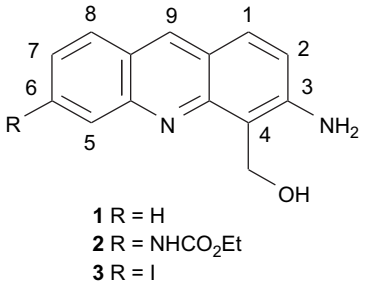

Fig. 1. Ortho-hydroxymethylaminoacridines.

which do not inhibit any topoisomerase, are nevertheless active and the images obtained by confocal microscopy with compound **1** were compatible with a localization into organelles such as lysosomes or mitochondria [2]. Because fluorescence emission can be strongly modified (even fully quenched) by interactions with biomolecules such as DNA, the dynamic secondary ion mass spectrometry (SIMS) imaging was used to demonstrate the absence of drug within the nucleus. SIMS imaging is based on the sputtering of secondary particles under the impact of high-energy primary ions. Upon the impact of these primary ions, most chemical bonds are broken and atoms or polyatomic fragments are ejected from the most superficial atomic layers of the specimen (1–2 nm thick), either as neutral or charged particles (ions). Ions can be selected by a mass spectrometer on the basis of their mass to charge ratio (m/z), while maintaining intact the topological information of their origin, thus leading to images representative of the spatial distribution of a specific ion within the sample surface (chemical mapping) [6,7].

The SIMS methodology requires in the molecule of interest either the presence of an atom, such as iodine, not found in living cells, or its labelling with a stable isotope, *e.g.* ^{13}C or ^{15}N, naturally occurring only in very weak concentration. Such modifications do not change (or hardly alter) the structure of the molecule and can be used to modify non-fluorescent compounds without the need of introducing bulky fluorescent reporter groups, which can deeply modify the intracellular drug distribution.

We thus chose to introduce an iodine atom at position C-6 of the acridine nucleus, as previous data [2] indicated that the antiproliferative activities were little influenced by the nature of the substituent present at that position.

As depicted in Scheme 1, the iodo analogue **3** was synthesized in three steps from 3-amino-6-iodoacridine **4**, itself prepared from proflavine as reported in the literature [8]. The key-step, formation of dihydrooxazinone **6** from carbamate **5**, involved the regioselective aromatic electrophilic substitution with formaldehyde and subsequent intramolecular transcarbamoylation. Ring opening in alkaline conditions yielded the reactive ortho-hydroxymethylamine **3**. It should be mentioned that iodo aromatic compounds become light and heat sensitive, which makes their purification delicate and lowers the yields.

To check that the presence of the iodine did not alter the biological properties, we first evaluated the antiproliferative effect against three human cancer cell lines (HT29, A549 and Hela) respectively derived from colon, lung and cervix cancer. As indicated in Table 1, introduction of the iodine has only a small influence on the IC_{50} value on the three cell lines. These data are consistent with results previously obtained [2]. This point was a prerequisite for using **3** as a labelled analogue of **1** for cellular uptake analysis.

Before studying the cell distribution by SIMS, we also checked by fluorescence microscopy that the presence of the iodine did not influence the cellular penetration and distribution. Very similar pictures were obtained for compound **1** and its iodo analogue **3** (data not shown). With these results in hand, we could perform the SIMS analysis.

The images obtained using SIMS technology are displayed in Fig. 2. As revealed in Fig. 2F, the iodine containing drug appears as bright spots within the cytoplasm, near the cell membrane, consistent with a vesicular accumulation. The intensity ratio is 50 to 1 between these hot spots and the rest of the cytoplasm, and 100 to 1 with the basal noise as well as with the nucleus, thus confirming the absence of **3** in the nucleus. Superposition of images 2E and 2F indicates a co-localization of the drug with protein rich organelles (as reflected by sulphur and iodine superposition). This result is fully compatible with previous results observed by confocal microscopy.

To confirm these results and to find in which organelles compound **3** is located, we used a technique on living cells, the real time fluorescence microscopy (Fig. 3). We chose this technology instead of the classical microscopy to preserve lysosome integrity. These organelles are sensitive to the fixation with PFA (paraformaldehyde) as demonstrated in previous experiments where we noticed a decrease of their fluorescence after fixation with PFA. The pictures obtained with compound **3** are collected in Fig. 3. Reference molecule **1** was studied for comparison.

As clearly shown in Fig. 3A–B and E–B, the two molecules, **1** and **3** are located in the cytoplasm near the cell membranes, with no detectable trace in the nucleus (no superposition with the blue nuclear marker). Superposition of the images indicates a co-localization of the drugs with lysosomal organelles (Fig. 3A–C and E–C) and not with the

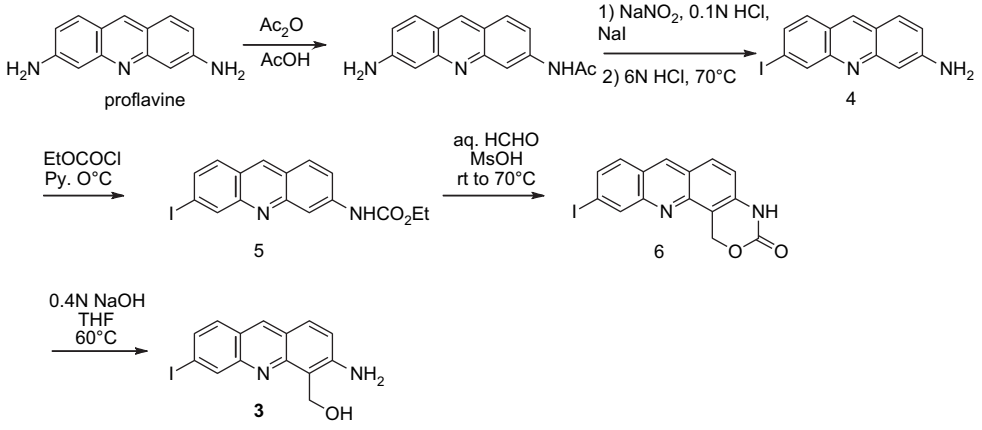

Scheme 1. Synthesis of the iodo analogue.

Table 1
In vitro antiproliferative activity (IC_{50}) against cancer cell lines expressed in nM.

Compound	IC_{50} (nM)[a]		
	HT29	Hela	A549
1	34 ± 9	70 ± 10	60 ± 7
3	70 ± 30	70 ± 30	130 ± 10

[a] IC_{50} values are the concentrations corresponding to 50% growth inhibition.

mitochondria (Fig. 3A–D and E–D). These results are fully compatible with what was observed using SIMS microscopy.

As we are in the presence of compounds that distribute in the lysosomes, we investigated if this localization would bring arguments on their possible mechanism of action. For these reasons, we analyzed the effects of compounds **1** and **3** on the cell cycle of the HT29 cell line after 24 and 48 h of treatment. The Fig. 4 shows that compounds **1** and **3** give similar profiles. These compounds lead first to an increase of the S phase for concentrations lower than 0.25 μM, then an increase of the sub-G1 phase for higher concentrations, at 24 and 48 h. These data correlate well with the absence of activity of compounds **1** and **3** on topoisomerases. The S phase partial arrest followed by the accumulation at sub-G1 phase may be related to the potent alkylating properties of this class of molecules, and indeed covalent binding to macromolecules (nucleic acids or proteins) would ultimately trigger apoptosis. Involvement of apoptotic pathway was further supported by PARP cleavage (data not shown).

3. Conclusion

The present results shed new light on the unusual cell distribution of cytotoxic 3-amino-4-hydroxymethyl acridine derivatives. Localization into the lysosomes is compatible with the results obtained by two innovative, powerful and complementary technologies, real time fluorescence microscopy and SIMS. To perform the SIMS analysis, we modified compound **1** by introducing an iodine atom at position 6. Replacing hydrogen by iodine has an impact on the lipophilicity of the molecule (calculated log P increases from 1.9 to 2.8), however the polar surface area, which is now recognized as a very useful descriptor for predicting cell distribution [9,10], remains constant (PSA = 59.1). Indeed, we have observed that *H*/*I* exchange does not significantly modify the biological properties (IC_{50} and sub-cellular localization). The cellular distribution of compound **1** shows a strong similarity with what was reported for the antitumor agent C1311 [11]. This compound, an imidazoacridone that was described as a DNA-binder and topoisomerase II inhibitor, also displayed a cytoplasmic localization in the lysosomes, and it was proposed that this lysosomotropic effect was determinant for the therapeutic efficacy of the drug. In recent articles, sequestration of active molecules into lysosomes and its cellular, biological and therapeutic consequences have been highlighted [12,13]. Associating a simple structure, fluorescence properties and potent antiproliferative activity, compound **1** makes an ideal candidate for further studies on the biological importance of lysosomes as antitumor drug targets. We also demonstrated that these novel technologies could be advantageously used for therapeutic development.

4. Experimental

4.1. Materials and methods

Melting points were determined using a Reicher Thermovar apparatus and are uncorrected. NMR spectra were recorded on Bruker AC 200 and AM 300 spectrometers using solvent as the internal reference (DMSO-d_6 at 2.49 ppm, $CDCl_3$ at 7.24 ppm); the chemical shifts are reported in ppm, in δ units. Mass spectra were recorded on a Polarisq Thermo Finnigan spectrometer. Elemental

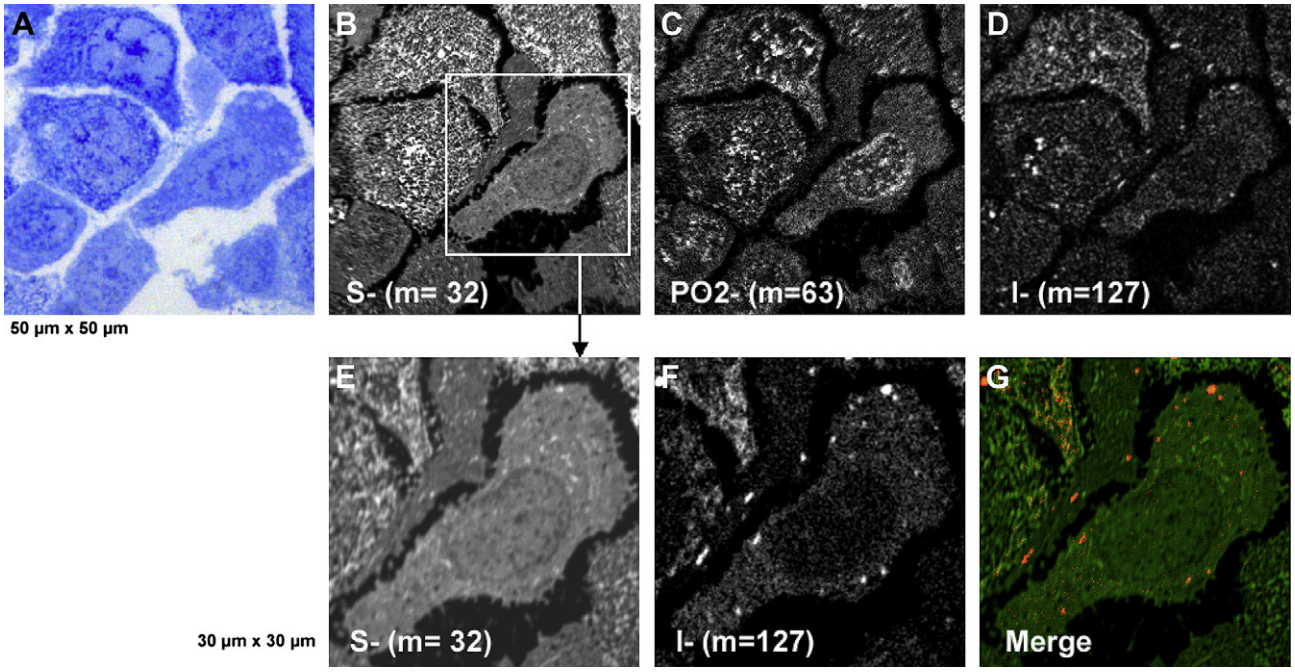

Fig. 2. Typical images of a thin section (0.4 μm) of HT29 cells incubated for 24 h with compound **3** (1 μM). First row, field of 50 μm × 50 μm, (A): optical image after staining with toluidine blue; (B–D) SIMS images: (B) sulphur ($m = 32$) giving an anatomical view of the cells, (C) phosphorus (PO_2^-, $m = 63$) underlying the nucleus contour, and (D) iodine ($m = 127$) showing the distribution of the drug. Second row, field of 30 μm × 30 μm, measurements at higher magnification of the area delimited by the white square in B showing SIMS image of sulphur (E), iodine (F) and the superposition (G) of images E and F.

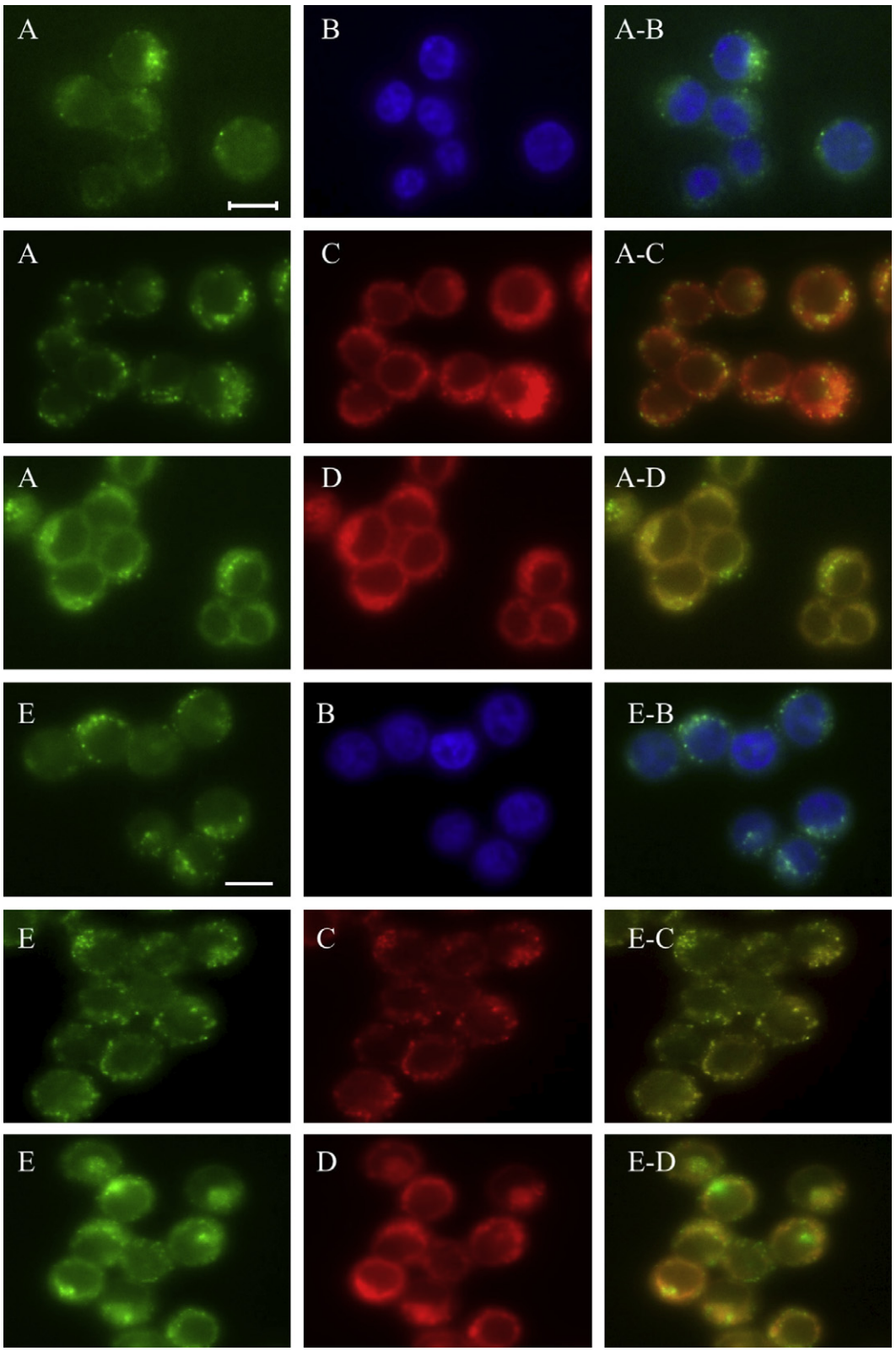

Fig. 3. Intracellular distribution of compounds **1** (A) and **3** (E) (10 μM each) in colorectal HT-29 cells, visualized by fluorescence microscopy (63×, scale: 10 μM) after 6 h of incubation. The blue (B) and red images (C–D) correspond to the subsequent incubation of the same cells with (B) nuclear marker DB75 (5 μM for 30 min at 37 °C), (C) LYSO Tracker Red (500 nM), and (D) MITO tracker Red (500 nM). The images with two letters correspond to the superimposed respective images.

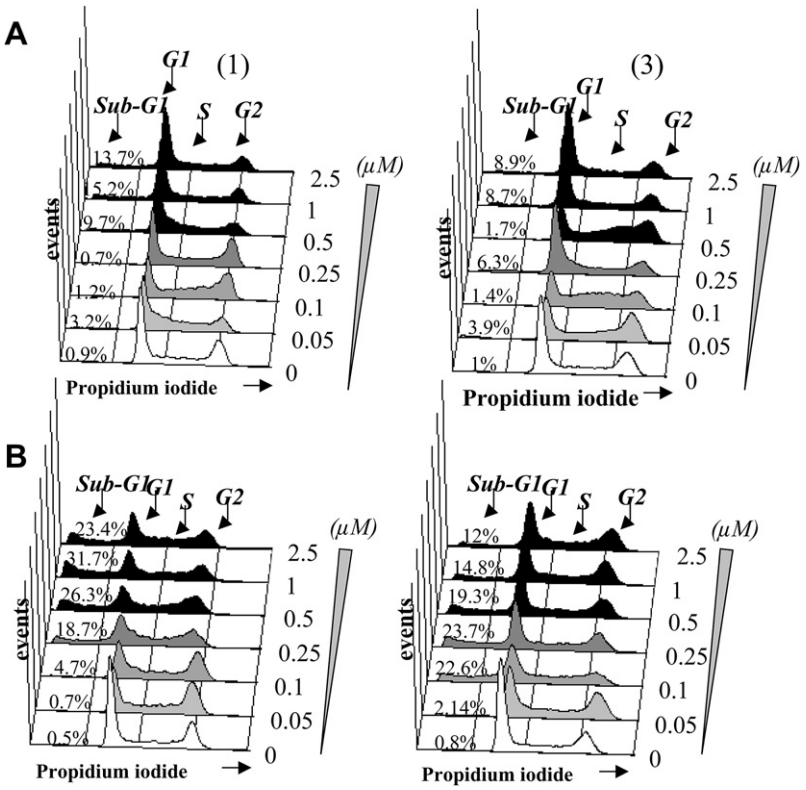

Fig. 4. Cell cycle analysis of HT-29 cells treated with graded concentrations of compound **1** (left column) and **3** (right column) for 24 h (A) and 48 h (B). Cells were analyzed with the FACScan flow cytometer as described in Materials and Methods. Percentage values correspond to the Sub-G1 population.

analyses were performed at "Service de microanalyse, Université Joseph Fourier". All starting materials were commercially available.

4.2. Synthesis

3-Amino-6-iodoacridine **4** was prepared from 3,6-diaminoacridine (proflavine) following published procedure [6].

4.2.1. 3-Ethoxycarbonylamino-6-iodoacridine (**5**)

Ethyl chloroformate (400 μL, 4.18 mmol) was added dropwise to a solution of 6-iodo-3-aminoacridine **4** (130 mg, 0.41 mmol) in pyridine (7 mL) cooled at 0 °C. The reaction was monitored by HPLC. When the reaction was completed after 3 h of stirring, pyridine was removed under reduced pressure. The residue was dissolved in aqueous NH_4OH and the resulting precipitate was filtered, washed with water until the filtrate showed a neutral pH. The compound **5** (141 mg, 89%) was thus obtained as a brown solid. An analytical sample was purified by chromatography on silica gel, with AcOEt as eluant. Mp: 145–148 °C, ^{1}H NMR (300 MHz, DMSO-d_6): δ 10.18 (s, 1H, NH), 8.97 (s, 1H, H-9), 8.52 (br s, 1H, H-5), 8.32 (br s, 1H, H-4), 8.07 (d, 1H, $J = 9.1$ Hz, H-1), 7.90 (d, 1H, $J = 8.8$ Hz, H-8), 7.78 (dd, 1H, $J = 1.6$, 8.8 Hz, H-7), 7.68 (dd, 1H, $J = 2.1$, 9.1 Hz, H-2), 4.23 (q, 2H, $J = 7.1$ Hz, CH_2), 1.31 (t, 3H, $J = 7.1$ Hz, CH_3). ^{13}C NMR (75 MHz, DMSO-d_6): δ 153.5 (C=O), 149.7 (C-4a), 149.1 (C-10a), 141.6 (C-3), 136.8 (C-5), 136.3 (C-9), 133.0 (C-7), 130.0 (C-8), 129.3 (C-1), 124.0 (C-8a), 123.0 (C-9a), 120.9 (C-2), 112.3 (C-4), 98.1 (C-6), 60.6 (CH_2), 14.4 (CH_3). HRMS (EI): $(M)^+_{found}$ 393.00996; $(M)^+_{calcd}$ for $C_{16}H_{14}O_2N_2I_1$ 393.00945.

4.2.2. 10-Iodo-1,4-dihydro-3H-[1,3]oxazino[4,5-c]acridin-3-one (**6**)

3-Ethoxycarbonylamino-6-iodoacridine **5** (50 mg, 0.13 mmol) was dissolved in 99% methanesulfonic acid (5 mL) in the presence of formaldehyde (37% aqueous solution, 91 μL, 1.09 mmol). The mixture was stirred at room temperature for 5 h and then heated at 70 °C for a further 12 h. The reaction was monitored by HPLC. When the reaction was completed, the mixture was allowed to cool to room temperature before being poured over 100 g of ice. The solution was carefully basified with aq. NH_4OH and extracted three times with AcOEt. The combined organic layers were washed with water until neutral pH, and then brine, dried over magnesium sulphate and evaporated under reduced pressure. This crude product was chromatographed on silica gel with a mixture of AcOEt/CH_2Cl_2 1:1 as eluant. The desired product **6** (25 mg, 52%) was thus obtained as a brown solid. Mp: 244–247 °C, ^{1}H NMR (300 MHz, DMSO-d_6): δ 10.57 (s, 1H, NH), 9.02 (s, 1H, H-7), 8.48 (br s, 1H, H-11), 8.09 (d, 1H, $J = 9.0$ Hz, H-6), 7.89 (d, 1H, $J = 8.8$ Hz, H-8), 7.79 (dd, 1H, $J = 1.6$, 8.8 Hz, H-9), 7.28 (d, 1H, $J = 8.9$ Hz, H-5), 5.91 (s, 2H, CH_2). ^{13}C NMR (75 MHz, DMSO-d_6): δ 150.9 (C-3), 148.7 (C-11a), 144.7 (C-12a), 138.2 (C-4a), 137.4 (C-7), 136.8 (C-11), 133.2 (C-9), 130.1 (C-6, C-8), 123.8 (C-7a), 123.0 (C-6a), 117.0 (C-5), 108.8 (C-12b), 98.9 (C-10), 66.0 (C-1). HRMS (EI): $(M)^+_{found}$ 376.97876; $(M)^+_{calcd}$ for $C_{15}H_{10}O_2N_2I_1$ 376.97815.

4.2.3. 3-Amino-4-hydroxymethyl-6-iodoacridine (**3**)

Compound **6** (33 mg, 0.09 mmol) was dissolved in a mixture of THF (10 mL) and aq. 0.4 N NaOH (3 mL). The reaction mixture was stirred in the dark at 60 °C for 10 h, then cooled to room temperature and left to stir over the week-end. The reaction was monitored by HPLC. When the reaction was completed, 50 mL of AcOEt was added to the solution. The aqueous phase was extracted twice with AcOEt. The combined organic layers were washed with water until neutral pH, and then brine. After drying over magnesium sulphate, the organic solvent was evaporated under reduced pressure. The resulting residue was poured into a mixture of diethyl

ether/pentane 1:1 and then filtered. Compound **3** (20 mg, 65%) was thus obtained as an orange solid. ^{1}H NMR (300 MHz, DMSO-d_6): δ 8.71 (s, 1H, H-9), 8.38 (br s, 1H, H-5), 7.79 (d, 1H, $J = 9.0$ Hz, H-1), 7.77 (d, 1H, $J = 8.6$ Hz, H-8), 7.62 (dd, 1H, $J = 1.6$, 8.6 Hz, H-7), 7.19 (d, 1H, $J = 9.0$ Hz, H-2), 6.18 (s, 2H, NH_2), 5.18 (s, 2H, CH_2). ^{13}C NMR (75 MHz, DMSO-d_6): δ 149.4 (C-4a), 149.2 (C-3), 148.4 (C-10a), 136.4 (C-5), 135.9 (C-9), 131.2 (C-7), 129.9 (C-8), 128.6 (C-1), 122.3 (C-8a), 121.9 (C-2), 121.2 (C-9a), 111.5 (C-4), 97.1 (C-6), 55.0 (CH_2). HRMS (EI): $(M)^+_{found}$ 350.99926; $(M)^+_{calcd}$ for $C_{14}H_{12}O_1N_2I_1$ 350.99888.

4.3. Organism culture and in vitro antiproliferative activity

Three human tumor cell lines were used and provided by American Type Culture Collection (Rockville Pike, MD). Cells (HT 29, Hela or A 549) were cultivated in Dulbecco's MEM supplemented with 10% fetal calf serum (FCS), 2 mM glutamine, 100 IU/mL penicillin, and 100 μg/mL streptomycin. All cells were grown at 37 °C in a humidified atmosphere containing 5% CO_2.

Cells from log-phase culture were seeded in 24-microwell plates (1 mL–5×10^{-4} cells/well) and incubated for two days. Tested compounds, in DMSO solution, were added under the minimum volume (5 μl) in increasing concentration. Control cells received 5 μl of DMSO alone. Plates were incubated 24 h, then medium was removed and cells washed twice with phosphate buffered saline before addition of fresh medium free of drug. Plates were reincubated for three days before evaluation of the cell survival by means of the MTT assay using 30 min incubation with 100 μg/well of 3-[4,5-dimethylthiazol-2-yl]-2,5-diphenyl tetrazolium bromide (MTT, Sigma). After removal of the medium, formazan crystals were taken up with 100 μl of DMSO and absorbance at 540 nm was measured with a microplate reader (Model 450 Bio-Rad), survival was expressed as % of the DMSO treated controls. All incubations were carried out at 37 °C in a water-jacketed CO_2 incubator (5% CO_2, 100% relative humidity). Cytostatic activity was expressed as IC_{50}, the concentration that reduced by 50% the number of treated cells relative to controls. IC_{50} values were extracted from regression curves obtained with experimental points.

4.4. SIMS imaging

HT29 cells were cultivated on Thermanox™ plastic film as described for antiproliferative activity. After two days, cells were exposed to compound **3** (1 μM) for 24 h and then rinsed four times in PBS before cryofixation as previously described by us [6,7]. Briefly, square pieces of the Thermanox film were fixed by slam-freezing on a metal mirror precooled at −180 °C and dehydrated by freeze-drying, in vacuum (0.2 Pa), starting at −110 °C and going progressively to −10 °C. Samples were then infiltrated by spurr's resin, with the temperature slowly increasing from −10° to 20 °C, and were subsequently polymerized at 65 °C. Serial sections of 0.4 μm were deposited either on stainless steel disks for SIMS analysis or on glass slides for light microscopy. SIMS analysis was performed using a NanoSIMS-50™ ion microprobe (CAMECA, Genevilliers, France) with a 16 KeV primary cesium ion beam. The probe was 100 nm in diameter, with an intensity of 1.5 pA. Fields of 50 μm × 50 μm to 30 μm × 30 μm were scanned over the surface of the sample in a 256 × 256 pixel raster. Depending upon the analysis, the dwell time ranged from 5 to 30 ms per pixel. The magnetic field was set to detect $^{127}I^-$ on the largest-radius detector. Under these conditions, the simultaneous detection of $^{31}P^-$ and $^{32}S^-$ was not possible because of the spacing limitation between detectors. Therefore, the distribution of phosphorus was obtained by acquisition of $^{31}P^{16}O_2^-$ ions. Images of $^{12}C^{14}N^-$, $^{32}S^-$, $^{31}P^{16}O_2^-$ and $^{127}I^-$ were acquired simultaneously. Images of $^{12}C^{14}N^-$, $^{32}S^-$ and $^{31}P^{16}O_2^-$ provide morphological and chemical features of cells. $^{12}C^{14}N^-$ and $^{32}S^-$ mostly refer to protein molecules, while $^{31}P^{16}O_2^-$ is representative of the distribution of large phosphate-rich molecules, mainly nucleic acids, thus localizing nuclei. For each anion detected, the raw data are a 16-bit 256 × 256 pixel image resulting from the probe scanning over the observed area. The intensity of each pixel corresponds to the direct local measurement of the flux of secondary ions. Image processing was performed using Image J software [Rasband WS (1997–2007) ImageJ. http://rsb.info.nih.gov/ij], a public-domain Java program. All SIMS elemental images are presented in a log scale.

4.5. Real time fluorescence microscopy

Cells (40,000 cells/cm^2) were incubated at 37 °C with tested compounds, usually at 10 μM for 6 h unless otherwise stated. Cells were then rinsed with ice-cold PBS (5 min) then incubated with the fluorescent probes: MitoTracker Red CMXRos (Molecular Probes, invitrogen), mitochondrion marker at 500 nM; LysoTracker Red (Molecular Probes, Invitrogen), lysosomes marker at 500 nM; or DB75 (2,5-bis(4-amidinophenyl)furan, graciously obtained by Pr David Boykin from Atlanta, US), nucleus marker at 5 μM. Incubation durations were performed during 30 min at 37 °C in the dark. After three washing with ice-cold PBS (5 min), cells were put in an appropriate culture medium and directly visualized by real time fluorescence microscopy (time laps) using Leica microscope with a 63× oil objective. All experiments were performed three times.

4.6. Cell cycle analysis

Cells were washed in PBS, fixed in cold 70% ethanol and placed at −20 °C during 12 h. Then, cells were washed in PBS, stained with RNase (10 μg/mL) and PI (50 μg/mL) 30 min at 37 °C in the dark. Cell cycle determinations were performed on 104 cells using a Becton Dickinson fluorescence-activated cell analyzer and data were interpreted using CellQuest, Winmdi and Cyclred logiciel.

Acknowledgments

This work was done under the support of research grants (to P.P.) from the Association pour la recherche sur le cancer and from the Institut de Recherches sur le Cancer de Lille; the authors thank the Service Commun d'Imagerie Cellulaire de l'IMPRT (IFR114) for access to the fluorescence microscope. The authors thank Brigitte Baldeyrou and Christine Bal-Mahieu for their technical support.

References

[1] For a recent review, see P. Belmont, J. Bosson, T. Godet, M. Tiano, Anticancer. Agents Med. Chem. 7 (2007) 139–169.
[2] F. Charmantray, M. Demeunynck, D. Carrez, A. Croisy, A. Lansiaux, C. Bailly, P. Colson, J. Med. Chem. 46 (2003) 967–977.
[3] F. Charmantray, A. Duflos, J. Lhomme, M. Demeunynck, J. Chem. Soc. Perkin Trans 1 (2001) 2962–2968.
[4] M. Demeunynck, F. Charmantray, A. Martelli, Curr. Pharm. Des. 7 (2001) 1703–1724.
[5] W.A. Denny, Expert. Opin. Investig. Drugs 6 (1997) 1845–1851.
[6] J.L. Guerquin-Kern, F. Hillion, J.C. Madelmont, P. Labarre, J. Papon, A. Croisy, Biomed. Eng. Online 3 (2004) 10.
[7] J.L. Guerquin-Kern, T.D. Wu, C. Quintana, A. Croisy, Biochim. Biophys. Acta 1724 (2005) 228–238.
[8] R.F. .Martin, D.P. . Kelly, Aust. J. Chem. 32 (1979) 2637–2646.
[9] G.M.M. El Maghraby, A.C. Williams, B.W. Barry, Int. J. Pharm. 292 (2005) 179–185.
[10] P. Erlt, B. Rohde, P. Selzer, J. Med. Chem. 43 (2000) 3714–3717.
[11] A.M. Burger, T.C. Jenkins, J.A. Double, M.C. Bibby, Br. J. Cancer 81 (1999) 367–375.
[12] R. Castino, M. Démoz, C. Isidora, J. Mol. Recognit. 16 (2003) 337–348.
[13] A.M. Kaufmann, J.P. Krise, J. Pharm. Sci. 96 (2007) 729–746.